Dilated Deep Neural Architectures for Improving Retinal Vessel Extraction

Sathananthavathi V (sathananthavathi@gmail.com)
Mepco Schlenk Engineering College https://orcid.org/0000-0002-8732-8652
Indumathi G
Mepco Schlenk Engineering College

Research Article

Keywords: Retinal Color fundus images, deep neural network, dilation, Fully Convolved Neural Network, depth concatenation, Entropy Loss Function

Posted Date: April 26th, 2021

DOI: https://doi.org/10.21203/rs.3.rs-405993/v1

Dilated deep neural architectures for Improving Retinal vessel Extraction

SATHANANTHAVATHI V[1], INDUMATHI G[2]
[1,2]*Department of Electronics and Communication Engineering*
Mepco schlenk Engineering College Sivakasi, India
E-mail: sathananthavathi@gmail.com[1], gindhu@mepcoeng.ac.in[2]

Human eye is an absolute sensory organ for vision. Eye sight is entirely accomplished by the blood flow in retinal vessels in eye. Diseases such as diabetes retinopathy, hypertension and arteriosclerosis cause change in branching pattern and diameter of retinal blood vessels leading to blindness. These changes can be analyzed by segmenting retinal blood vessel. Hence the retinal vasculature is recognized as the promising anatomical region for the diagnosis of several commonly seen diseases including cardiovascular related and diabetes. In this paper we propose two novel deep neural architectures named as Dilated fully convolved convolutional neural network (FCNN) and dilated depth concatenated neural network (DCNN) to segment the retinal blood vessels. The feature maps of fundus images are extracted by multiple dilated convolutional layers and due to the large field of view by dilation, pixel classification gets improved. The proposed work is evaluated for both the proposed architectures with and without dilation. It is observed from the obtained results that dilation enhances the network performance. To eliminate the non-uniform illumination and low contrast differences effect the preprocessed images are used for training the architectures. The proposed methodologies are experimented on the two publicly available databases DRIVE and STARE database.

Keywords: Retinal Color fundus images, deep neural network, dilation, Fully Convolved Neural Network, depth concatenation, Entropy Loss Function

1. INTRODUCTION

Primary requirement for screening and diagnosis of retinal diseases involves segmentation of retinal blood vessels. Two dimensional or three dimensional colour fundus images are used for segmenting retinal vessel. In early days analyst or experts manually segment the retinal vessel from the fundus images which is a time consuming progress and it leads to error. Automatic segmentation of retinal blood vessels reduces time and it helps in early detection and diagnosis of diseases. Improvement in computer aided system leads to development of various methods for retinal vessel segmentation. Several supervised or unsupervised methods have already been proposed for retinal vessel segmentation. Supervised methods rely on manual annotation groundtruth for segmentation of retinal vessel whereas unsupervised method does not depend on manual annotation. .

Salazar Gonzalez et al. proposed an unsupervised graph cut based retinal vessel segmentation method [1] in which the input images are preprocessed by adaptive histogram equalization and distance transform. Recently, retinal vessel segmentation based on Frangi enhancement filter [2], ICA enhancement technique based method [3] and also line detector based methodology [4], are also proposed. Influence of significant features need to be considered for the vessel extraction are mentioned in the optimization based feature selection method [5] for the retinal vessel segmentation. Zhu et al. proposed an unsupervised method [6] by taking thirty nine discrete features for each fundus image comprising morphological feature, hessian feature and so on. The extracted feature together with groundtruth is given as input to the extreme machine learning classifier and the image is classified as vessel and non-vessel region. In many approaches the feature selection for segmentation of image is strenuous task as segmented result depends on features selected. Convolutional neural network selects the best feature for processing the image. High efficiency of neural network based methods lead to its implication for medical image processing. Fu et al. proposed neural network based retinal vessel segmentation method [7] in which Convolutional neural network learns the features and generates probability map and segment the vessel by pixel concurrence using conditional random field. Zhexin et al. proposed transfer learning base approach [8] for retinal vessel segmentation and then the obtained result are post processed to improve the accuracy of segmented result. In [9] Olaf et al. proposed neural network architecture for segmenting medical images. The architecture consists of multiple hidden layers; the output of each hidden stage is up sampled and concatenated to previous layer output before upsampling. Dasgupta et al. [10] proposed a method for segmentation of retinal vessel in which input images are preprocessed by extracting green channel of fundus image to remove non

uniform illumination and then the image is divided into patches and trained using fully convolved neural network. The images are then classified using probability map by setting threshold. In [11] sumathi et al. proposed a robust algorithm for segmentation of retinal vessels. The input images are preprocessed to normalize the illumination and contrast problem and thirteen dimension feature vectors are extracted. Probability map are formed using neural network classifier and the images are classified as vessel region and non-vessel region. In [12] Shelhamer et al. proposed a transfer learning approach for retinal vessel segmentation using Alexnet. The conventional fully connected layer and classification layer on the output layer are modified to form a fully convolutional neural network. Orlando et al. [13] segmented the retinal colour fundus images using convolutional neural network for feature extraction and classified the image using SVM (state vector machine) classifier. The input images are preprocessed to eliminate the contrast and illumination problem.

In [14] Liskowski et al. proposed a deep neural network based approach in which the input images are preprocessed with global contrast normalization. The neural network is trained with four thousand samples which are data augmented using geometric transformation and gamma correction. In addition to the above surveys, several deep learning based methods [15-17] are also proposed for retinal blood vessel extraction. In [18], Qiaoliang et al. proposed a cross modality approach for retinal vessel segmentation. Mapping function is used to obtain the corresponding vessel map. The neural network consists of five layers viz, one input layer, output layer and three hidden layers with a sigmoid activation function consisting of 756 units. The neural network is trained with green channel image and it is transformed to vessel label. Olivera et al. [19] proposed a method for retinal vessel segmentation in which multiscale analysis is performed by combining Stationary wavelet transform and fully convolutional neural network. The green channel of the images is taken and is its mean and variance is normalized. The remaining channels are stationary wavelet transformed and are then trained using neural network.

In the proposed work, retinal vessels are segmented by two convolutional neural network architectures. The contribution of the proposed work includes the development of dilated fully convolved neural network and dilated Depth concatenated neural network architectures for the retinal vessel extraction. The retinal fundus images are preprocessed and are trained to detect the vasculature by the dilated architectures in a supervised manner.

2. PROPOSED METHODOLOGY

2.1 Outline

In the proposed work two different architectures of neural networks are proposed one is derived from segnet architecture [25] and it is named as fully convolved convolutional neural network (FCCN), the other is derived from unet architecture [9] and it is named as depth concatenated neural network (DCNN). The neural network consists of input layer, hidden layer for feature extraction and output layer for classification. Both the proposed architecture consists of five stages of encoder and decoder layers. All the convolutional layers in the proposed architecture are replaced by dilated convolutional layer. The ultimate significance of the dilated convolution is the large field of observation. It is inferred from our experimentation that convolution computed using the non-local neighbor pixels improves the classification performance.

In this work, the input images are preprocessed to eliminate illumination and low contrast between vessels and background. Features are extracted using multiscale CNN and are classified as vessel and non-vessel region using pixel classification. The vessel region is less compared to non-vessel region this leads to imbalance of pixel count between vessel and non-vessel region. The imbalance of pixel count is eliminated by cross entropy loss function thereby reducing misclassification of classes.

2.2 Preprocessing

Non uniform illumination and low contrast difference between vessels and non-vessels lead to improper segmentation of vessel. Retinal color fundus images are preprocessed to eliminate contrast and illumination problem. The green channel of the fundus image provides better contrast and can reduce illumination problem hence it is considered as the input image. The extracted green channel fundus images are further preprocessed for vessel enhancement. In the proposed work Contrast limited adaptive histogram equalization (CLAHE) is applied for vessel enhancement. CLAHE is a local enhancement technique that limits the amplification of histogram by clipping at a predefined value. To enable the vascular region more visible, CLAHE is the most commonly used technique in medical

images. The preprocessed fundus image is shown in figure 1.

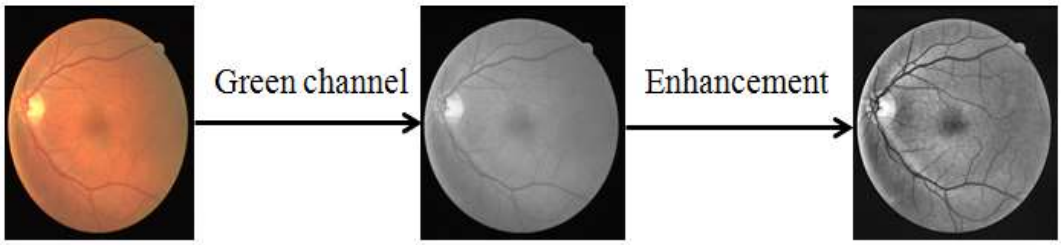

Fig. 1. Preprocessed image

2.3 Dilated convolution

Dilated convolution differs from conventional convolution layer by providing space between variables in kernel during convolution operation [26]. Dilation enlarges the receptive field without increasing the quantity of parameters or computation. The dilated convolution operation is given in equation 1.

$$(F *_l k)(p) = \sum_{s+lt=} F(s)K(t) \quad (1)$$

In dilated convolution, a kernel of size k x k filter is enlarged to a filter of size k + (k-1) (r-1), where r is the dilated rate. It keeps the same resolution by allowing adaptable aggregation of the multiscale information. The pictorial representation of dilation working principle with 3x3 filter is shown in figure 2.

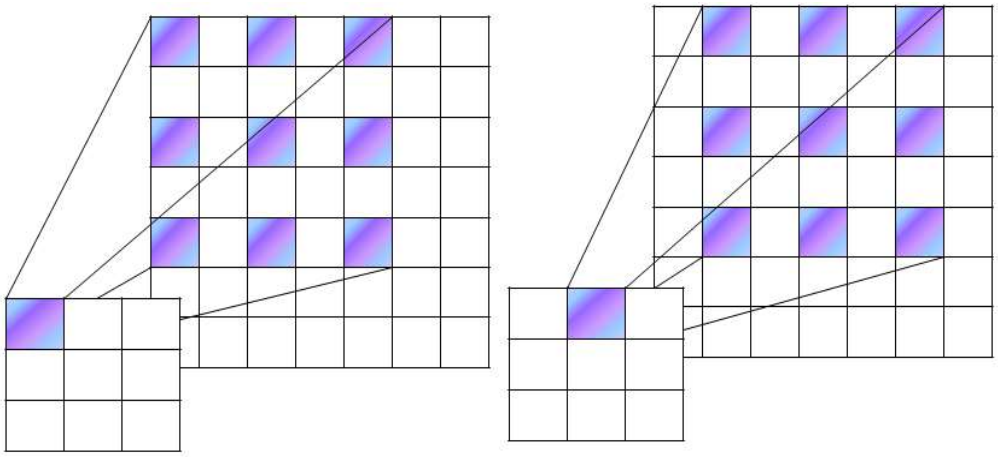

Fig. 2. Dilated convolution

2.4 Fully convolutional Neural Network

The proposed FCCN architecture is extracted from segnet architecture [25], which consists of five stages of encoder and decoder containing twenty six layers of convolution with two convolution layers in the first two stages of encoder and decoder and three in the next three stages with constant kernel size 7x7. The proposed FCCN architecture consists of five stages of encoder and decoder and it is shown in figure 3. All the stages of encoder consist of two dilated Convolution layer, each convolution layer is followed by batch normalization and rectified linear unit. Convolution operation performed in the proposed FCCN involves dilated filter of 3x3 with striding and padding of one. Batch normalization layer are included to increase the speed of training and rectified linear unit is used as the activation function. The output of each encoder hidden stage is unpooled and is convolved twice. Pooling indices of unpooling layer is extracted from the encoder stage and using those indices the unpooling operation is done on the decoder stage. The number of filters in each layer remains the same throughout the stage. The maximum pooling operation of 2x2 is performed in the proposed FCCN. The output layer consists of softmax and pixel classification layer. The softmax layer assigns probability value for each class in an image. The pixel classification layer classifies the image as vessel

and non-vessel region. The proposed architecture contains totally 73 layers comprising batch normalization and activation function layer; Increase of network layer enhances the architecture to learn significant features to segment the retinal vessels. Each layer provides useful information required for segmentation at various levels of features. The last convolution is a 1x1 convolution to map the channel to be the same as the input number of channels. The layer description of encoder and decoder for the proposed FCCN architecture are given in table 1.

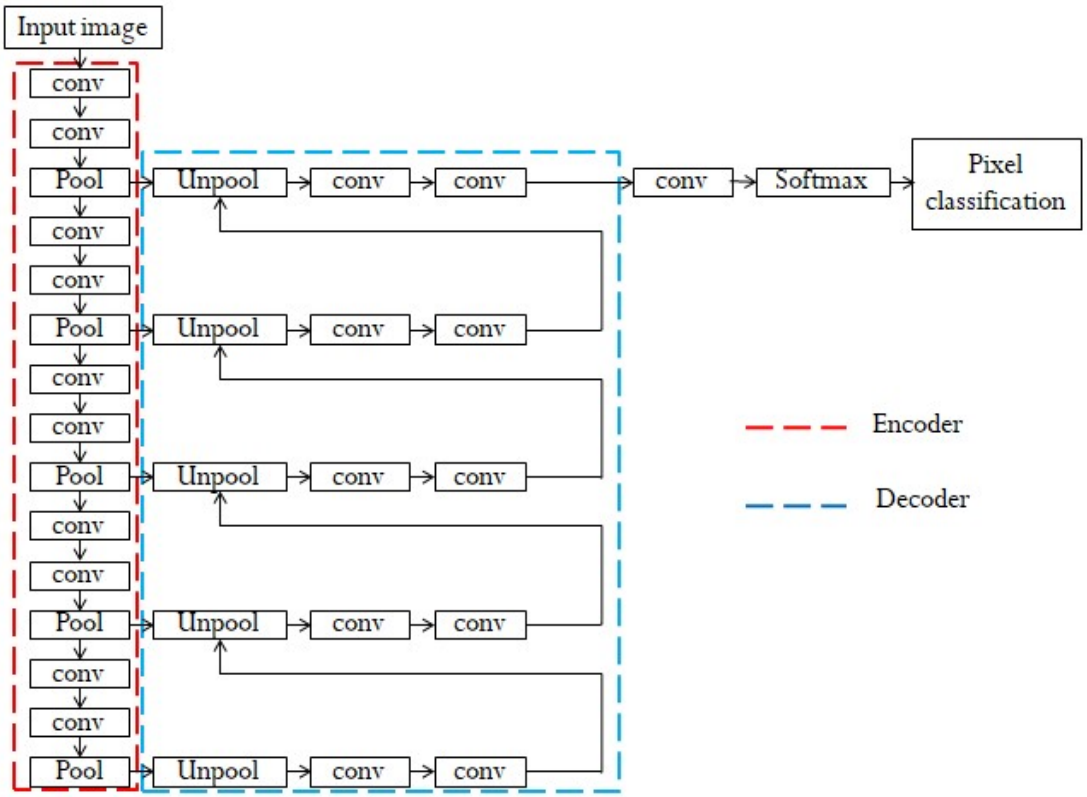

Fig .3 Fully convolved neural network

Table 1 Encoder and decoder layer specification and output image size for FCCN

Encoder Layer	Filter Size And Channel	Input Image Size	Output Image Size
1-CONV 1	3x3,64	512x512	512x512
1-CONV 2	3x3, 64	512x512	512x512
Max Pooling	2x2, 64	512x512	256x256
2-CONV 1	3x3, 64	256x256	256x256
2-CONV 2	3x3, 64	256x256	256x256
Max Pooling	2x2, 64	256x256	128x128
3-CONV 1	3x3, 64	128x128	128x128
3-CONV 2	3x3,64	128x128	128x128
Max Pooling	2x2,64	128128	64x64
4-CONV 1	3x3,64	64x64	64x64
4-CONV 2	3x3, 64	64x64	64x64
Max Pooling	2x2, 64	64x64	32x32
5-CONV 1	3x3, 64	32x32	32x32
5-CONV 2	3x3, 64	32x32	32x32
Max Pooling	2x2, 64	32x32	16x16

Decoder Layer	Filter Size And Channel	Input Image Size	Output Image Size
Unpool	-	16x16	32x32
5-CONV 1	3x3,64	32x32	32x32
5-CONV 2	3x3, 64	32x32	32x32
Unpool	-	32x32	64x64
4-CONV 1	3x3, 64	64x64	64x64
4-CONV 2	3x3, 64	64x64	64x64
Unpool	-	64x64	128x128
3-CONV 1	3x3,64	128x128	12x128
3-CONV 2	3x3,64	128x128	128x128
Unpool	-	128x128	256x256
2-CONV 1	3x3,64	256x256	256x256
2-CONV 2	3x3,64	256x256	256x256
Unpool	-	256x256	512x512
1-CONV 1	3x3, 64	512x512	512x512
1-CONV 2	3x3,64	512x512	512x512

2.5 Depth Concatenated Neural Network

The proposed DCNN architecture is modified from Unet architecture [9]. The hidden layer of DCN architecture consists of dilated convolution layer, maxpooling layer, ReLu layer, batch normalization layer, depth concatenation layer and upconvolutional layer. The proposed architecture is shown in figure 4.

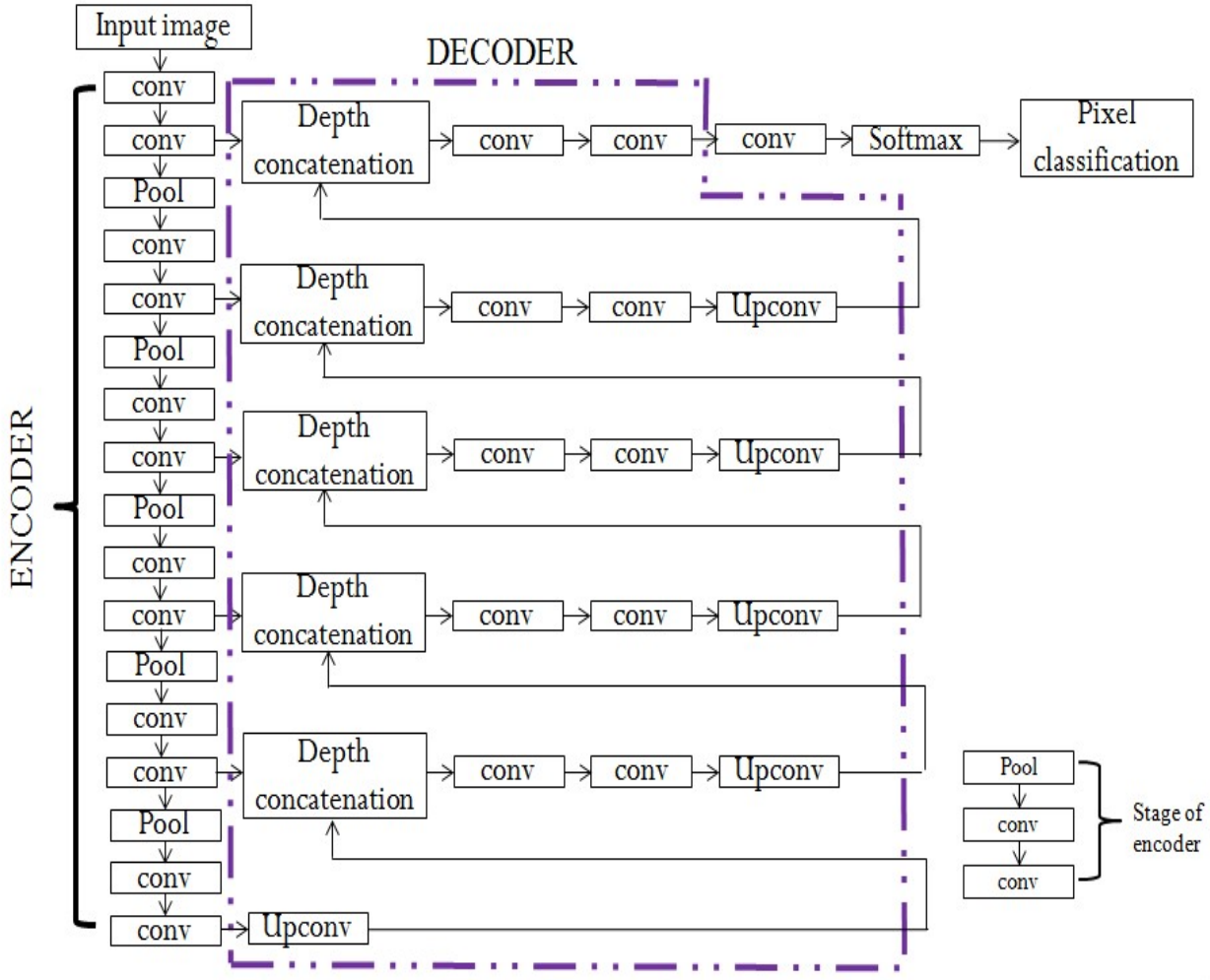

Fig. 4. Depth Concatenated Neural Network

The hidden layers form five encoder stages and five decoder stages. Each encoder stage consists of two convolutional layer and maxpooling layer. The depth concatenation layer in the proposed work concatenates the output from the encoder stage to the corresponding decoder stage. The depth concatenation layer concatenates the two inputs that are of same height and width. The difference between the proposed architecture and the UNET architecture is that all the dropout layers are removed and batch normalization after each convolution layer is included and convolution layer used in each stage is dilated convolution. The upconvolution layer performs transpose convolution operation. The decoder stage consists of depth concatenation layer, two convolution layer and one upconvolution layer. The number of filters with which the images convolved in each stage doubles that of previous stage. The number of filter in the first stage is sixteen and hence for the fifth stage it is 512. The size of image is reduced to half the size of image for each encoder stage. The images are then upsampled by decoder. Convolution operation performed in the proposed work involves dilation factor of 2. The pooling operation performed in the proposed work is 2x2 maximum pooling.

The output layer in DCN is same as that of FCCN. The encoder and decoder layer specifications are listed in table 2.

Table 2 Encoder and decoder layer specification and output image size for DCNN

Encoder Layer	Filter Size And Channel	Input Image Size	Output Image Size
1-CONV 1	3x3,16	512x512	512x512
1-CONV 2	3x3,16	512x512	512x512
Max Pooling	2x2,16	512x512	256x256
2-CONV 1	3x3,32	256x256	256x256
2-CONV 2	3x3,32	256x256	256x256
Max Pooling	2x2,32	256x256	128x128
3-CONV 1	3x3,64	128x128	128x128
3-CONV 2	3x3,64	128x128	128x128
Max Pooling	2x2,64	128128	64x64
4-CONV 1	3x3,128	64x64	64x64
4-CONV 2	3x3,128	64x64	64x64
Max Pooling	2x2,128	64x64	32x32
5-CONV 1	3x3,256	32x32	32x32
5-CONV 2	3x3,256	32x32	32x32
Max Pooling	2x2,256	32x32	16x16

Decoder Layer	Filter Size And Channel	Input Image Size	Output Image Size
TCONV	2x2,256	16x16	32x32
5-CONV 1	3x3,256	32x32	32x32
5-CONV 2	3x3,256	32x32	32x32
5-TCONV	2x2,128	32x32	64x64
4-CONV 1	3x3,128	64x64	64x64
4-CONV 2	3x3,128	64x64	64x64
4 -TCONV	2x2,64	64x64	128x128
3-CONV 1	3x3,64	128x128	12x128
3-CONV 2	3x3,64	128x128	128x128
3 -TCONV	2x2,32	128x128	256x256
2-CONV 1	3x3,32	256x256	256x256
2-CONV 2	3x3,32	256x256	256x256
2 -TCONV	2x2,16	256x256	512x512
1-CONV 1	3x3,16	512x512	512x512
1-CONV 2	3x3,16	512x512	512x512

2.6 Class Imbalance problem

In pixel classification layer, all the pixels in the input images are classified as vessels and non-vessels. Vessel pixel count occupies less than one fourth of the total image pixel count which leads to misclassification of vessel as non-vessel. In order to avoid this class imbalance problem class weightage of vessel is increased. The images are classified as vessel and non-vessel, whose corresponding weights are denoted as $cw = cw^{(1)}, cw^{(2)}$. The total class weight ($T(CW)$) is given by equation (2)

$$T(CW) = cw^{(1)} + cw^{(2)} \tag{2}$$

Class frequency are obtained by dividing each class weight by total class weight. Class frequency F is presented by equation (3)

$$F^{(i)} = \frac{cw^{(i)}}{T(cw)} ; \quad i=1,2 \tag{3}$$

Inverse class weight ($cw_I^{(i)}$) is obtained by taking inverse of class frequency and is given by equation (4).

$$cw_I^{(i)} = \frac{1}{F^{(i)}} ; \quad i=1,2 \tag{4}$$

Pixel classification layer is updated with class weight so that more weightage is given to the vessel region compared to the non vessel region. The network learns well by avoiding the class imbalance problem with the inclusion of weightage to the classes and it enhances the segmentation result.

3. RESULTS AND DISCUSSION

3.1 Database

The proposed methodology is experimented using two popular databases namely DRIVE (Digital Retinal Images for Vessel Extraction) [30] and STructured Analysis of Retina (STARE) [31]. Canon CR5 with 45° field of view is used for capturing DRIVE images. The database comprises totally 40 images; half the images are for training images and the half is for testing purpose. Each image is of size 565x584, and available with corresponding groundtruth and its mask image. Two ground truths are provided for testing; two experts were developed the groundtruth. Testing images are also available with one mask image. The STARE database are obtained using TopCon TRV-50 fundus camera at 35° Field of view. Images are of size 605x700 and for each image two independent manual segmentations are offered as groundtruth.

3.2 Evaluation metric

The proposed methodology is evaluated using sensitivity, specificity and accuracy as performance metrics. The classified pixels may be under any of the following cases; True Positive (TP), True Negative (TN), False Positive (FP), False Negative (FN). TP is the outcome of vessel predicted correctly as vessel and those are wrongly predicted as non-vessel pixels instead of vessels are counted as FN. TN is the outcome of non-vessel pixel correctly predicted as non-vessel and the non-vessel pixel wrongly predicted as vessel are defined as FP. The sensitivity (Se), specificity (Sp) and accuracy (Acc) are calculated as follows.

$$Se = \frac{TP}{TP+FN} \tag{5}$$

$$Sp = \frac{TN}{TN+FP} \tag{6}$$

$$Acc = \frac{TP+TN}{TP+TN+FN+FP} \tag{7}$$

3.3 Experimental Results

The proposed Dilated FCNN and DCNN architectures are trained using twenty training images taken from DRIVE database and is evaluated for the remaining twenty test images. In addition in order to validate the performance of the proposed trained architecture we tested twenty abnormal images from STARE database. In order to show the improvement in accuracy for the proposed dilated architectures, we do experimentation on both the architectures with and without dilation layers. The entire experimentation is carried out on Intel i5 core, 32GB CPU system using Matlab 2018b. The number of epoch is a parameter that defines the number of times the training algorithm learns the entire training dataset. Both the proposed architectures are trained until the training accuracy improvement and loss reaches an optimum value; that is further improvement is very negligible. It is experiential that the training accuracy and training loss for FCCN architecture is 95.71% and 0.001 respectively. The DCNN architecture reaches the training accuracy of about 92.35% and loss of 0.131. Even though training accuracy is more for FCNN architecture, overall accuracy computation is better for DCNN architecture. Also it is observed that when all the convolutional layers are replaced by dilated convolutional layers, the overall accuracy gets increased for both FCNN and DCNN architectures. The improvement in overall accuracy for the dilated architectures is due to the decline of false positives more accurately by the proposed architectures. The segmented results for DRIVE database using FCCN and DCNN with and without dilation are shown in figure 5.

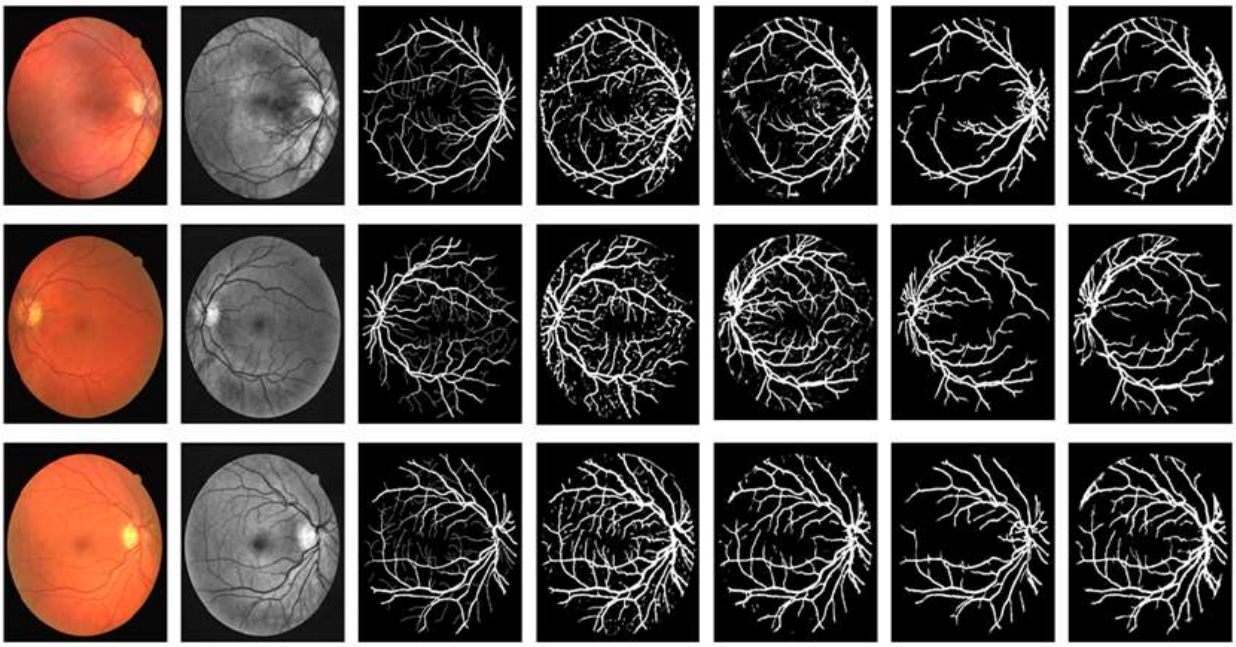

Fig. 5. Segmentation result of DRIVE dataset with dilation. (a) Color fundus image. (b) Enhanced green channel fundus image. (c)Ground truth. (d) FCCN (e) DCNN (f) FCCN with dilation (g) DCNN with dilation

Table 3**.** Evaluation Metrics of DRIVE database for FCCN and DCN

Image	FCCN architecture			DCNN architecture		
	Sensitivity%	Specificity%	Accuracy%	Sensitivity%	Specificity%	Accuracy%
1	77.67	96.44	93.97	80.86	96.99	95.61
2	76.78	96.81	93.80	80.92	96.93	95.31
3	82.86	96.73	94.81	86.89	95.70	95.02
4	72.23	97.11	93.74	83.74	96.44	95.44
5	66.84	97.54	93.31	84.40	95.91	95.04
6	68.51	98.13	93.89	84.32	95.54	94.68
7	69.62	97.17	93.47	78.61	96.42	94.93
8	61.05	98.02	93.34	83.85	96.13	95.29
9	57.87	98.64	93.78	85.29	96.23	95.56
10	71.48	96.91	93.83	82.20	96.76	95.71
11	89.85	95.93	95.13	73.42	96.58	94.48
12	67.87	97.54	93.77	82.88	96.40	95.43
13	72.19	97.24	93.64	86.96	95.73	95.06
14	73.35	96.34	93.61	80.28	96.98	95.72
15	76.72	96.34	94.01	70.99	97.96	95.74
16	70.04	97.67	94.00	81.51	96.82	95.56
17	74.02	97.93	94.24	83.30	96.47	95.56
18	70.68	97.26	94.16	78.22	97.49	95.97
19	84.55	96.96	95.44	79.03	97.80	96.14
20	73.12	97.31	94.70	77.25	97.71	96.18
Average	**72.87**	**97.20**	**94.03**	**81.25**	**96.65**	**95.42**

Table 4. Evaluation Metrics of DRIVE database for FCCN and DCN with dilation

Image	FCCN architecture with dilation			DCNN architecture with dilation		
	Sensitivity%	Specificity%	Accuracy%	Sensitivity%	Specificity%	Accuracy%
1	83.96	96.08	95.00	77.41	97.15	95.71
2	85.18	96.62	95.45	84.09	96.77	95.68
3	70.75	97.10	94.47	81.66	96.75	95.71
4	77.62	97.54	95.70	86.38	96.97	96.25
5	75.77	97.62	95.57	79.02	97.91	96.47
6	72.32	97.58	95.12	81.48	97.45	96.26
7	78.24	97.20	95.47	77.97	97.18	95.76
8	69.77	97.97	95.54	86.44	97.25	96.58
9	75.88	97.69	95.92	80.75	98.31	97.24
10	79.55	97.08	95.64	77.21	97.71	96.36
11	77.71	96.63	94.94	79.13	97.53	96.22
12	77.49	97.22	95.52	83.07	97.41	96.46
13	80.20	96.81	95.19	74.07	98.06	96.16
14	77.44	97.16	95.57	78.14	97.43	96.17
15	85.37	96.45	95.65	84.14	96.38	95.68
16	82.27	96.75	95.44	78.65	97.35	95.97
17	77.61	97.01	95.38	72.51	98.01	96.24
18	81.48	96.51	95.32	80.33	97.08	96.00
19	87.57	96.17	95.45	85.88	96.69	95.97
20	82.12	96.59	95.53	81.19	97.19	96.23
Average	**78.91**	**96.99**	**95.39**	**80.48**	**97.33**	**96.16**

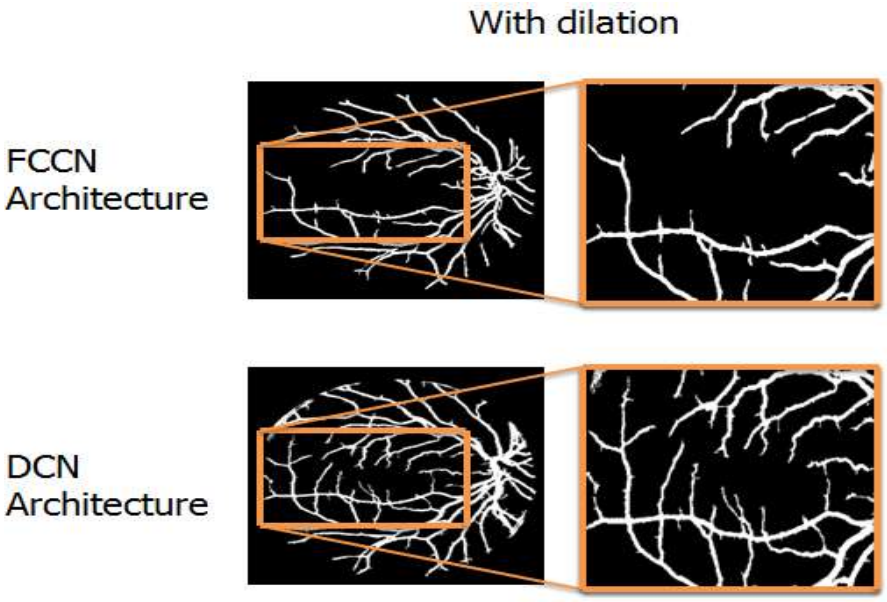

Fig. 6. Comparison of segmented result between FCCN and DCNN architectures

İn order to verify the data independancy of the proposed architectures, the vessel extracted from the image with different levels of contrast and illumination are listed. In Fig.5, the first row shows the result of low contrast image, the result of high illuminated image in second row and the result of high illuminated and low contrast image in third row using the proposed architectures with and without dilation. The evaluation metric for twenty test images of DRIVE such as sensitivity, specificity and accuracy are calculated and tabulated in table 3 and for dilation it is tabulated in table 4. First human observer groundtruth is taken to perform the metric calculation.

The evaluation metric obtained for DCNN architecture is better compared to FCNN architecture. The accuracy value of DCNN is increased to nearly one percentage compared to FCCN. From table 3 and 4 it is observed that both architectures with dilated convolution layers have improved accuracy and sensitivity value. The visibility of the vessel extracted image is good for the DCNN dilated architecture due to the avoidance of artifacts arised due to retinal image capturing effects. The maximum sensitivity, specificity and accuracy for twenty images of DRIVE database for Dilated FCNN are 87.57%, 97.97% and 95.92% respectively. The maximum sensitivity, specificity and accuracy for twenty images of DRIVE database for Dilated DCNN is 89.44%, 98.31% and 97.24%. The comparison of segmented image of two Dilated architectures are shown in figure 6. From the figure shown, it is clearly identified that the segmented result obtained using DCNN with dilation are better compared to FCNN with dilation. Thin vessels are correctly distinguished from the background by the dilated convolutional layers of DCNN.

The cross validation of the proposed FCCN and DCNN is done using STARE database (i.e) the network is trained using DRIVE database and is tested on STARE database. The abnormal images form STARE database are purposely selected for cross validation. The segmented result for STARE database are shown in figure 7. The segmented result for the abnormal images also found good for Dilated DCNN compared to other architectures.

Table 5. Evaluation Metrics of STARE database for FCCN and DCNN

Image	FCCN architecture			DCNN architecture		
	Sensitivity%	Specificity%	Accuracy%	Sensitivity%	Specificity%	Accuracy%
1	66.15	92.91	91.84	72.92	96.56	94.83
2	72.36	94.52	93.02	89.90	93.22	92.88
3	79.02	94.1	93.37	89.47	94.07	93.60
4	46.4	96.22	93.42	90.53	92.41	92.21
5	85.1	90.85	90.6	86.85	90.85	90.44
6	86.76	92.53	92.5	58.26	98.78	92.56
7	90.77	89.15	89.51	87.60	94.26	93.69
8	85.27	90.38	90.32	87.54	92.14	91.73
9	85.86	89.84	90.08	89.90	91.68	91.50
10	88.3	89.47	89.74	64.84	99.50	95.11
11	95.23	89.42	89.66	95.45	96.92	96.80
12	95.16	89.12	89.52	92.21	94.02	93.87
13	85.16	91.04	90.82	96.47	97.31	97.23
14	84.37	91.33	91.23	89.65	94.27	93.83
15	65.51	92.64	91.98	96.01	95.74	95.76
16	65.49	93.14	91.23	85.56	90.35	89.83
17	92.24	91.5	91.45	90.84	93.97	93.66
18	73.7	95.36	94.81	90.57	95.04	94.61
19	57.03	94.34	93.84	91.72	95.71	95.38
20	53.6	95.26	93.36	90.62	93.19	92.96
Average	**77.67**	**92.16**	**91.62**	**86.84**	**94.50**	**93.62**

From figure 7, it is observed that the abnormalities like red and bright lesions present in the input images are eliminated in a better way by the proposed architectures. The evaluation metric for twenty test images of STARE using both architecture with dilation such as sensitivity, specificity and accuracy are calculated and tabulated in tables 5 and 6. The maximum sensitivity, specificity and accuracy of STARE database for FCCN with dilation are 95.58%, 98.55% and 96.31% respectively. The maximum sensitivity, specificity and accuracy of STARE database for DCNN with dilation is about 95.16%, 98.98% and 98.07%. From the tables, it is observed that overall performance of DCNN architecture is better than FCCN architecture. It is also observed that sensitivity value get improved for the dilated covolution architecture compared to the conventional architecture. Figure 8, shows the comparison of performance metrics for the FCNN and DCNN architectures with and without dilation. It is inferred that accuracy and specificity value improved for the Dilated DCNN architecture. Even the sensitivity value is reduced to 80% for the Dilated DCNN, it is still high among most of the existing methodologies.

Table 6. Evaluation Metrics of STARE database for FCCN and DCNN with dilation

Image	FCCN architecture			DCNN architecture		
	Sensitivity%	Specificity%	Accuracy%	Sensitivity%	Specificity%	Accuracy%
1	76.88	94.33	91.93	87.96	97.85	97.01
2	67	95.76	94.09	90.1	97.48	96.67
3	79.26	94.44	93.45	89.7	98.25	97.31
4	52.43	98.55	94.49	90.62	96.71	96.02
5	87.55	92.87	92.12	87.82	99.25	98.07
6	92.01	92.87	92.41	90.08	97.1	96.38
7	94.76	91.42	91.36	89.45	95.92	95.18
8	89.34	92.85	92.24	92.77	96.17	95.76
9	93.65	93.14	92.52	89.63	95.98	95.31
10	93.63	93.5	93.05	94.57	95.2	95.15
11	94.1	91.13	91.45	93.48	95.26	95.12
12	95.58	92.19	92.44	90.99	97.35	96.82
13	88.15	93.85	93.03	94.04	95.62	95.47
14	90.07	94.36	93.4	86.24	96.24	95.27
15	83.22	94.91	92.19	95.16	94.81	94.84
16	71.63	96.81	93.45	85.68	98.98	97.55
17	90.74	93.11	93.02	89.43	92.9	92.57
18	82.19	97.6	96.31	90.84	95.06	94.61
19	79.95	97.74	95.86	90.94	95.9	95.38
20	62.31	94.84	93.24	91.63	94.51	94.2
Average	**83.22**	**94.31**	**93.1**	**89.25**	**96.34**	**95.64**

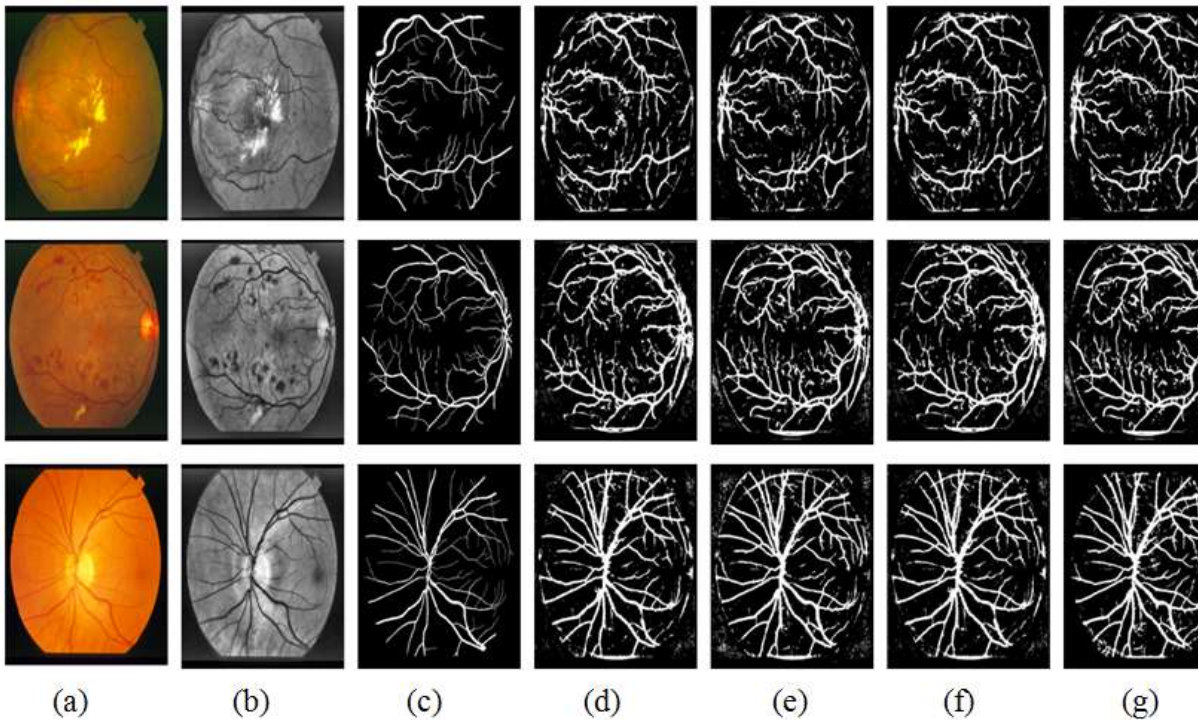

Fig. 7. Segmentation result of STARE database a) Color fundus image. (b) Enhanced green channel fundus image. (c) Ground truth. (d) FCCN (e) DCNN (f) FCCN with dilation (g) DCNN dilation

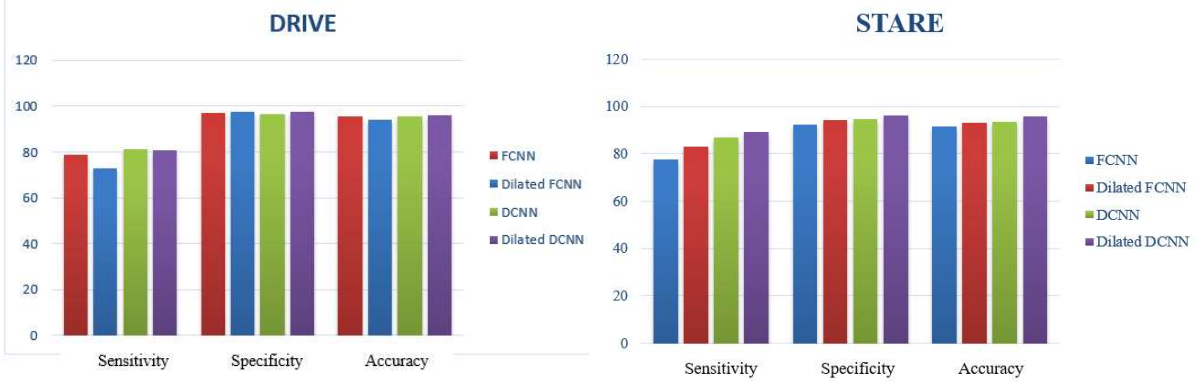

Fig 8. Bar graph comparison of evaluation metric

In order to verify the significance of dilation in convolution layers, the proposed architectures are compared with some of the existing Deep neural network (DNN) architectures and other recent methods. The performance comparison of DRIVE database with existing methodologies is listed in Table 7 and it is inferred that the proposed depth concatenated dilated architecture results are better compared to most of the existing methods. We also do experimentation on the data independency of the proposed architecture. The dilated architectures which are trained on normal images from DRIVE database is tested over selected abnormal images from STARE database. Sensitivity achieved by the depth concatenated dilated architecture is about 89.25% and as far as we know, it is the maximum sensitivity obtained for the retinal vessel extraction for STARE database. Crossed trained STARE database also shows better compared to the existing methodologies and they are listed in Table 8. Accuracy and sensitivity of the Dilated DCNN architecture shows better performance compared to other methods.

Table 7. Performance Comparison with existing methodologies for DRIVE

Publication year	Method	Accuracy	Sensitivity	Specificity
2018	Shahid [2]	0.958	0.730	0.9793
2018	Soomro [3]	0.953	0.752	0.976
2018	Biswal [4]	0.9541	0.71	0.97
	DNN based Methods:			
2016	Li [14]	0.9527	0.7569	0.9816
2016	Liskowski [10]	0.9515	0.752	0.9806
2018	Oliveira [15]	0.9576	0.8039	0.9804
2018	Jiang [11]	0.9624	0.754	0.9825
2018	Yan [12]	0.9542	0.7653	0.9818
2018	Hu [13]	0.9533	0.7772	0.9793
2020	**Proposed DNN:**			
	Dilated FCNN	0.9539	0.7891	0.9699
	Dilated DCNN	0.9616	0. 8048	0.9733

Table 8. Performance Comparison with existing methodologies for STARE

Publication year	Method	Accuracy	Sensitivity	Specificity
2011	Marin[32]	0.9526	0.6944	0.9819
2012	Fraz [33]	0.9495	0.7010	0.9770
2016	Li [14]	0.9545	0.7027	0.9828
2018	Oliveira [15]	0.9597	0.8453	0.9726
2020	**Proposed DNN:**			
	Dilated FCNN	0.931	0.8322	0.9431
	Dilated DCNN	0.9564	0.8925	0.9634

4.2 Conclusion

Extraction of fine vessels from the retinal fundus images are still a challenging task. İn this work, we proposed two novel deep neural neural netwoks based on dilated convolution layers. Dilated convolution performs well in the vessel detection task irrespective of vessel thickness. İt is also inferred that for the pixel level classification, depth concatenation with dilated convolution improves the result in a better way. The proposed architectures are observed to be the optimum performing architctures due to the inclusion of class balanced cross entropy loss function. The proposed dilated architectures optimized the segmentation of retinal blood vessels. The proposed methodology is evaluated on DRIVE and STARE database using the two different proposed architectures. The fine vessels are detected well in the DCNN with dilation architecture compared to FCNN architecture. In future the work can be further improved by enhancing encoder and decoder layers. The proposed dilated architectures show superior performance in the fine vessel detection even in the presence of abnormalities. İn conclusion, based on the performance measures calculated and also by the naked eye observation proposed architectures outperform the state of art methods.

Acknowledgment:

Authors would like to acknowledge Principal and Management of Mepco Schlenk Engineering College, Sivakasi for their encouragement and support for this research work

Compliance with Ethical Standards:

Conflict of Interest : Authors Sathananthavathi.V & Indumathi.G declare that they have no conflict of interest.
Ethical approval: This article does not contain any studies with human participants performed by any of the authors.

REFERENCES

1. A. Salazar-Gonzalez , D. Kaba , Y. Li , X. Liu , "Segmentation of the blood vessels and optic disk in retinal images, " IEEE J. Biomed. Health Inf. 18 (6) (2014) 1874–1886.
2. Shahid, M., Taj, I.A. (2018). Robust retinal vessel segmentation using vessel's location map and Frangi enhancement filter, IET Image Process., 12(4): 494–501.
3. Soomro,T.A., Khan, T.M., Khan, M.A.U., et al. (2018). Impact of ICA-based image enhancement technique on retinal blood vessels segmentation, IET Image Process., 6: 3524–353
4. Biswal, B., Pooja, T., Bala Subrahmanyam, N. (2018). Robust retinal blood vessel segmentation using line detectors with multiple masks, IET Image Process., 12(3): 389–399.
5. V.Sathananthavathi, G.Indumathi (2018) BAT algorithm inspired retinal blood vessel segmentation, IET image processing, 12(11): 2075-2083
6. C. Zhu , B. Zou , R. Zhao , J. Cui , X. Duan , Z. Chen , Y. Liang , Retinal vessel segmentation in colour fundus images using extreme learning machine, Comput. Med. Imag. Graph. 55 (2017) 68–77.
7. Huazhu Fu , Yanwu Xu , Damon Wing Kee Wong ,Jiang Liu , "Retinal vessel segmentation via deep learning and conditional random field," in Proc. MICCAI, 2016, pp. 132-139.
8. Zhexin Jiang, HaoZhang, YiWang, Seok-BumKo , "Retinal blood vessel segmentation using fully convolutional network with transfer learning," Computerized Medical Imaging and Graphics Volume 68, September 2018,
9. Olaf Ronneberger, Philipp Fischer, Thomas Brox, " U-net Convolutional neural networks for biomedical image segmentation,"in Proc. MICCAI, pp. 234-241, 2015
10. A. Dasgupta, and S. Singh, "A fully convolutional neural network basedstructured prediction approach towards the retinal vessel segmentation,"in Proc. ISBI, 2017, pp. 18-21.
11. Sumathi T Vivekanandan P Ravikanth Balaji, " Retinal Vessel Segmentation using Neural Network (RVSNN)," Volume 12, Issue 5, May 2018, p. 669 – 678
12. Shelhamer, E., Long, J., Darrell, T., 2017. "Fully convolutional networks for semantic segmentation," IEEE Trans. Pattern Anal. Mach. Intell. 39 (4), 640–651
13. J.I. Orlando, E. Prokofyeva, M.B. Blaschko, "A discriminatively trained fully connected conditional random field model for blood vessel segmentation in fundus images," IEEE Transaction on Biomedical Engineering vol 64
14. Paweł Liskowski, Krzysztof Krawiec,Member, "Segmenting Retinal Blood Vessels with DeepNeural Networks, " IEEE Transactions on Medical Imaging (Volume: 35 , Issue: 11 , Nov. 2016
15. Xiaohong Wang, Xudong Jiang, Jianfeng Ren. (2019). Blood vessel segmentation from fundus image by a cascade classification framework, Pattern Recognition. 88:331-341.
16. Zengqiang Yan, Xin Yang, Kwang-Ting Cheng. (2018). Joint Segment-Level and Pixel-Wise Losses for Deep Learning Based Retinal Vessel Segmentation, IEEE Transactions On Biomedical Engineering, 65(9): 1912-1923.
17. Kai Hu, Zhenzhen Zhang, Xiaorui Niu, Yuan Zhang, Chunhong Cao, Fen Xiao, Xieping Gao (2018). Retinal vessel segmentation of color fundus images using multiscale convolutional neural network with an improved cross-entropy loss function, Neurocomputing. 309: 179-191.
18. Qiaoliang Li, Member, IEEE, Bowei Feng, LinPei Xie, Ping Liang, Huisheng Zhang, and Tianfu Wang, " A Cross-Modality Learning Approach forVessel Segmentation in Retinal Images, " IEEE Transactions on Medical Imaging Volume: 35 , Issue: 1 , Jan. 2016
19. Americo Oliveira, Sergio Pereira Carlos A.Silva, " Retinal vessel segmentation based on Fully Convolutional Neural Networks, " Expert Systems with ApplicationsVolume 112, 1 December 2018, Pages 229-242
20. S.A. Salem, N.M. Salem, A.K. Nandi, "Segmentation of retinal blood vessel using a novel clustering algorithm (RACAL) with a partial supervision strategy", Med. Biol. Eng. Comput. 45 (3) 2007, 261–273.
21. S. Wang, Y. Yin, G. Cao, B. Wei, Y. Zheng, G. Yang, " Hierarchical retinal blood vessel segmentation based on feature and ensemble learning", Neurocomputing 149 (PB) 2015 708–717.

22. D. Marín, A. Aquino, M.E. Gegúndez-Arias, J.M. Bravo, “A new supervised method for blood vessel segmentation in retinal images by using gray-level and moment invariants based features”, IEEE Trans. Med. Imag. 30 (1) 2011 146–158.
23. Y. Yin et al., “Automatic segmentation and measurement of vasculaturein retinal fundus images using probabilistic formulation,” Computational and mathematical methods in medicine, vol. 2013.
24. M. M. Fraz et al., “Retinal vessel extraction using first-order derivativeof gaussian and morphological processing,” in Advances in Visual Computing. Springer, 2011, pp. 410–420.
25. Vijay Badrinarayanan., “Segnet: A deep convolutional encoder-decoder architecture for image segmentation,” in IEEE Transaction on pattern analysis and machine learning, vol 39, No 12 December 2017.
26. Marios et. al. “Semantic Segmentation of Pathological Lung Tissue with Dilated FullyConvolutional Networks,” IEEE journal of biomedical and health informatics, vol. 23, no. 2, march 2019.
27. J.J. Staal, M.D. Abramoff, M. Niemeijer, M.A. Viergever, B. van Ginneken, "Ridge based vessel segmentation in color images of the retina", *IEEE Transactions on Medical Imaging*, 2004, vol. 23, pp. 501-509.
28. A. Hoover, V. Kouznetsova and M. Goldbaum, "Locating Blood Vessels in Retinal Images by Piece-wise Threhsold Probing of a Matched Filter Response", *IEEE Transactions on Medical Imaging*, vol.19 no.3, pp. 203-210, March 2000.
29. Zhendong Zhang, Xinran Wang and Cheolkon Jung, “DCSR: Dilated convolutions for single image super-resolution,” IEEE transactions on image processing, vol 28, No 4. April 2019
30. Xiaomeng Li, Hao Chen, Xiaojuan Qi, Qi Dou, Chi Wing Fu, “H-Dense Unet:Hybrid densely connected unet for liver and tumor segmentation from CT volumes, ” IEEE transaction on medical imaging, Vol 37, No 12 December 2018
31. Ruirui Li, Wenjie Liu, Lei Yang, Shihao Sun, Wei Li, “DeepUnet:A deep fully convolutional network for pixel-level sea segmentation,” IEEE journal of selected topics in applied earth observation and remote sensing Vol 11, no 11, November 2018
32. Diego Marin, Arturo Aquino, Manuel Emilio Gegundez-Arias, Jose Manuel Bravo, “A New Supervised Method for Blood Vessel Segmentation in Retinal Images by Using Gray-Level and Moment Invariants-Based Features,” IEEE Transactions On Medical Imaging, Vol. 30, No. 1, January 2011
33. Fraz, M. M., Remagnino, P., Hoppe, A., Uyyanonvara, B., Rudnicka, A. R., Owen, C. G., & Barman, S. A, “An ensemble classification-based approach applied to retinal blood vessel segmentation,” IEEE Transactions on Biomedical Engineering, Vol 59 no. 9, 2538–2548, 2012.

Author’s biography

Sathananthavathi Vallikutti is an Assistant professor (Sr.Grade) in ECE, Mepco Schlenk Engineering College. She obtained her B.E from Madurai Kamaraj University and M.E from Anna university in 2003 and 2010 respectively. She completed her Ph.D. on retinal image processing under Anna University. She is a lifetime member of ISTE and IETE. Her interests encompass medical image processing and optimization techniques.

Indumathi Ganesan is a professor in ECE, Mepco Schlenk Engineering College. She obtained her B.E and M.E from Madurai Kamaraj University in 1990 and 1998 respectively. She received Ph.D. from Anna University. She is a lifetime member of ISTE and IETE. Her interests encompass several aspects of wireless communications such as Signal and Image processing, antenna design.

Figures

Figure 1

Preprocessed image

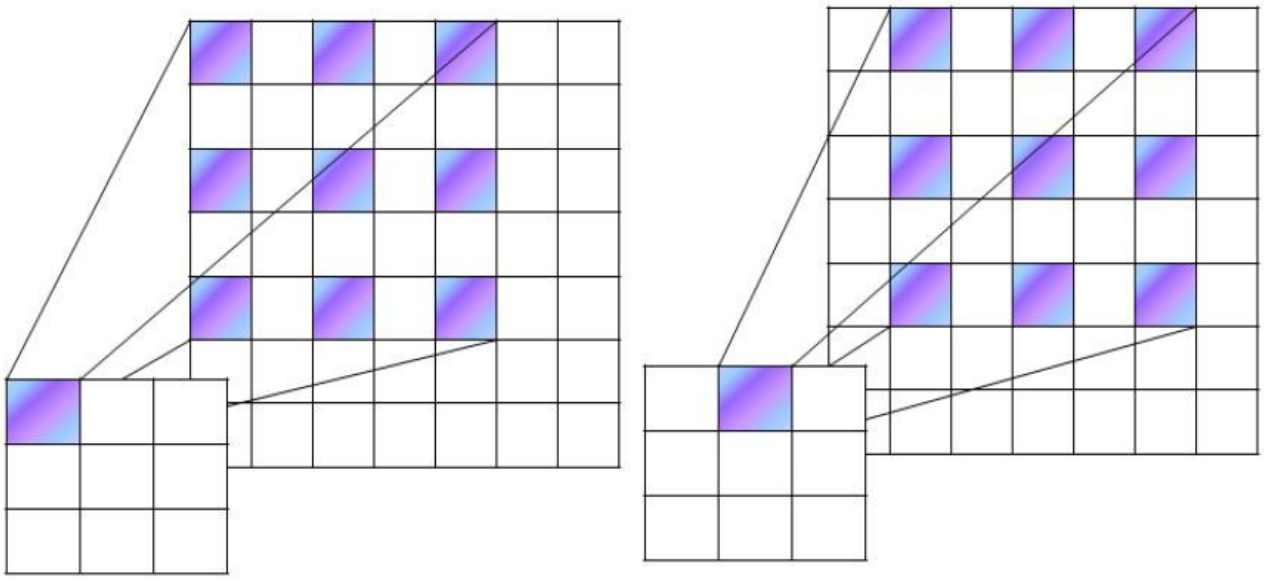

Figure 2

Dilated convolution

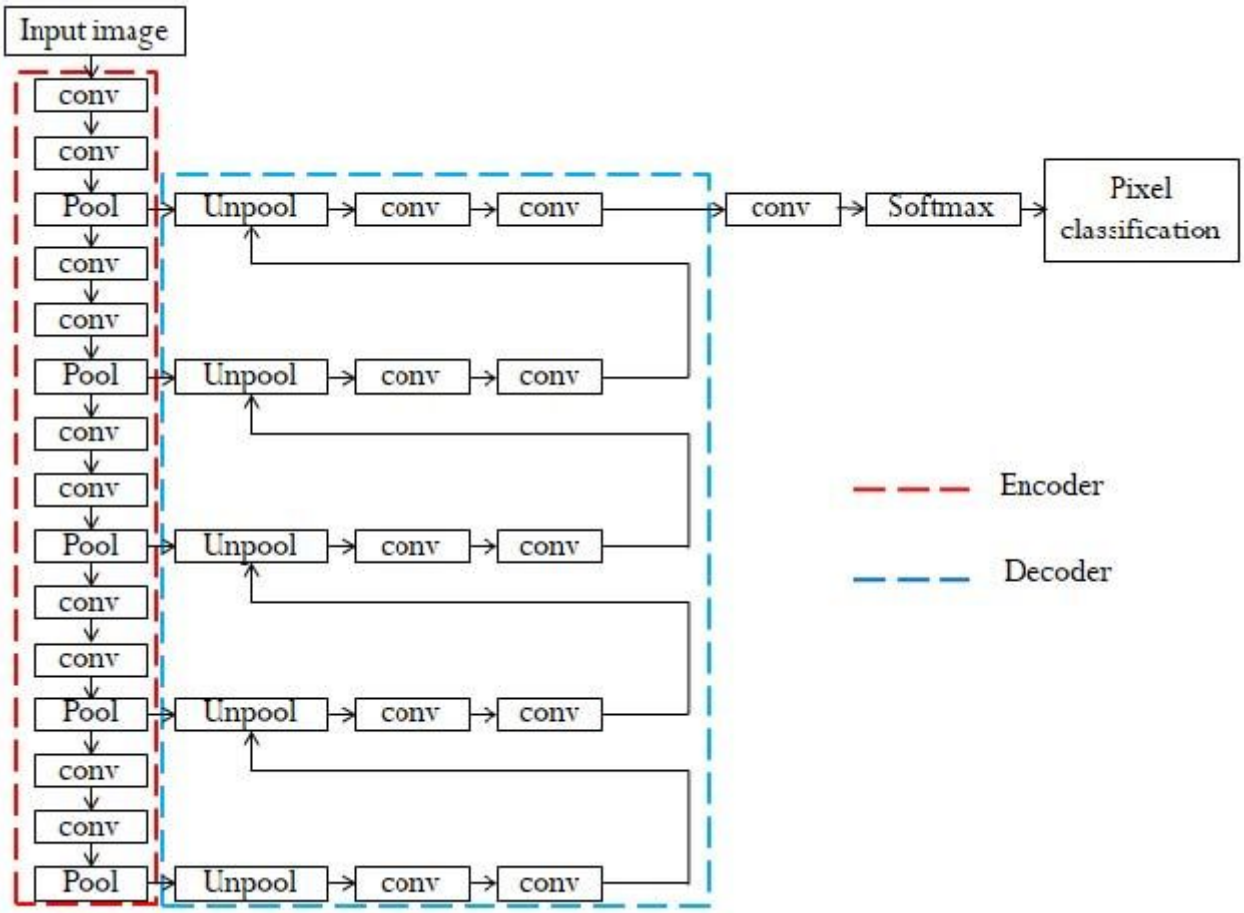

Figure 3

Fully convolved convolutional neural network

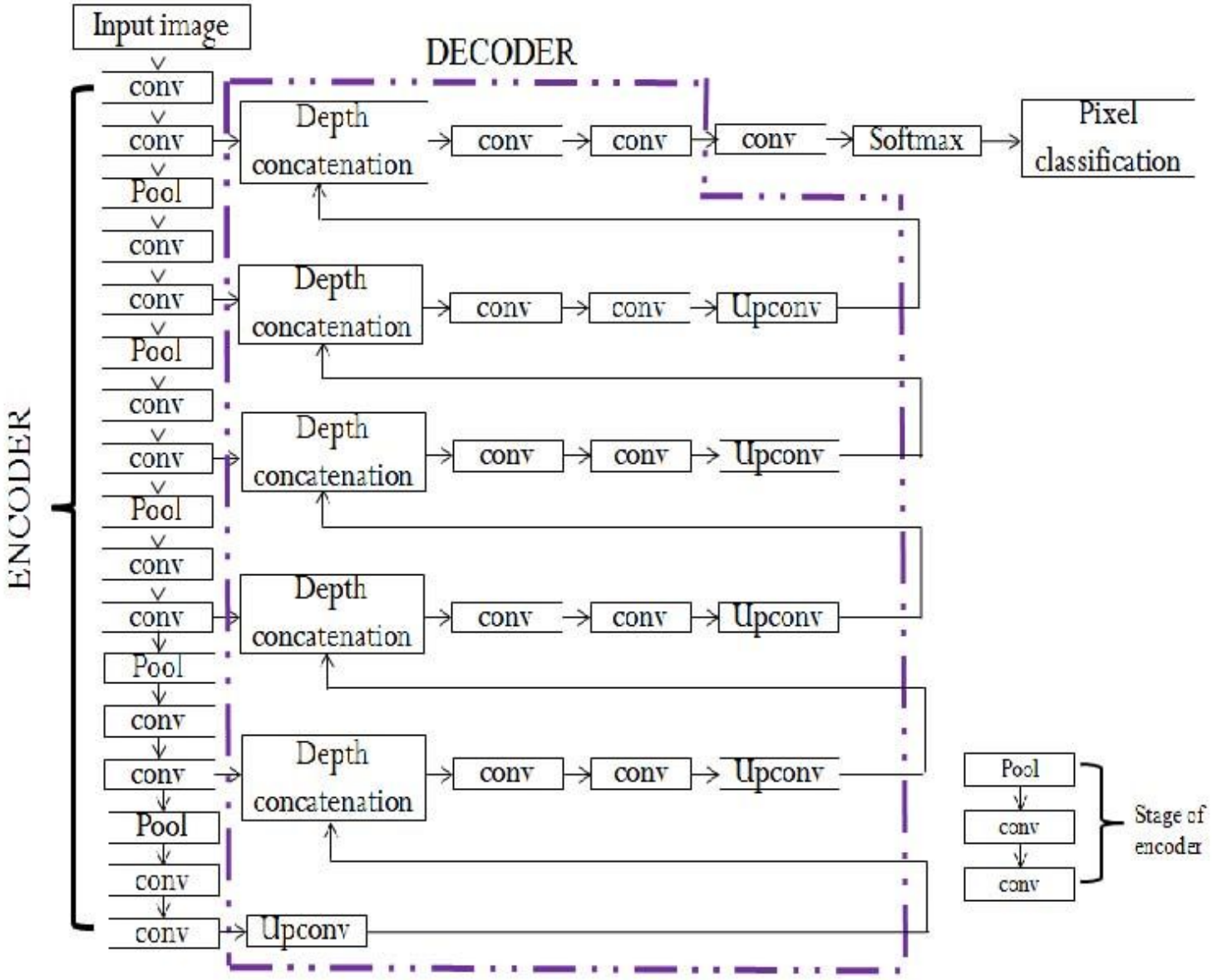

Figure 4

Depth Concatenated Neural Network

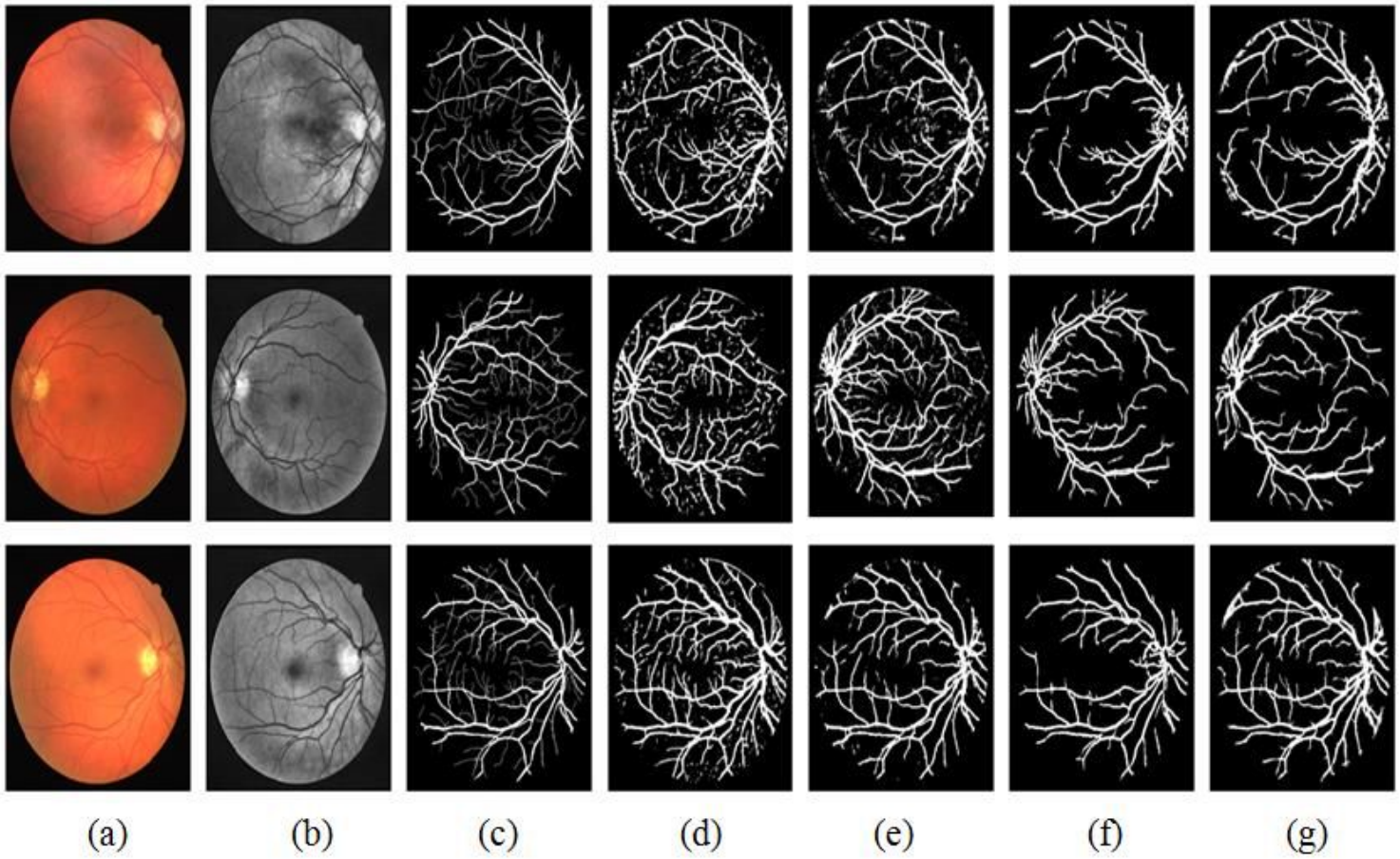

Figure 5

Segmentation result of DRIVE dataset with dilation. (a) Color fundus image. (b) Enhanced green channel fundus image. (c)Ground truth. (d) FCCN (e) DCNN (f) FCCN with dilation (g) DCNN with dilation

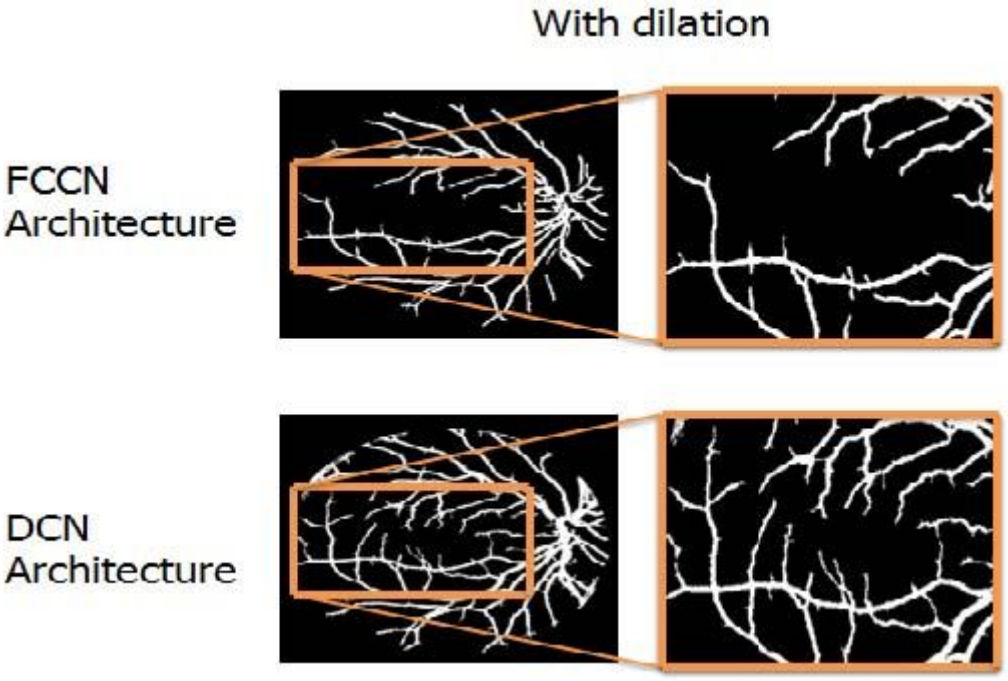

Figure 6

Comparison of segmented result between FCCN and DCNN architectures

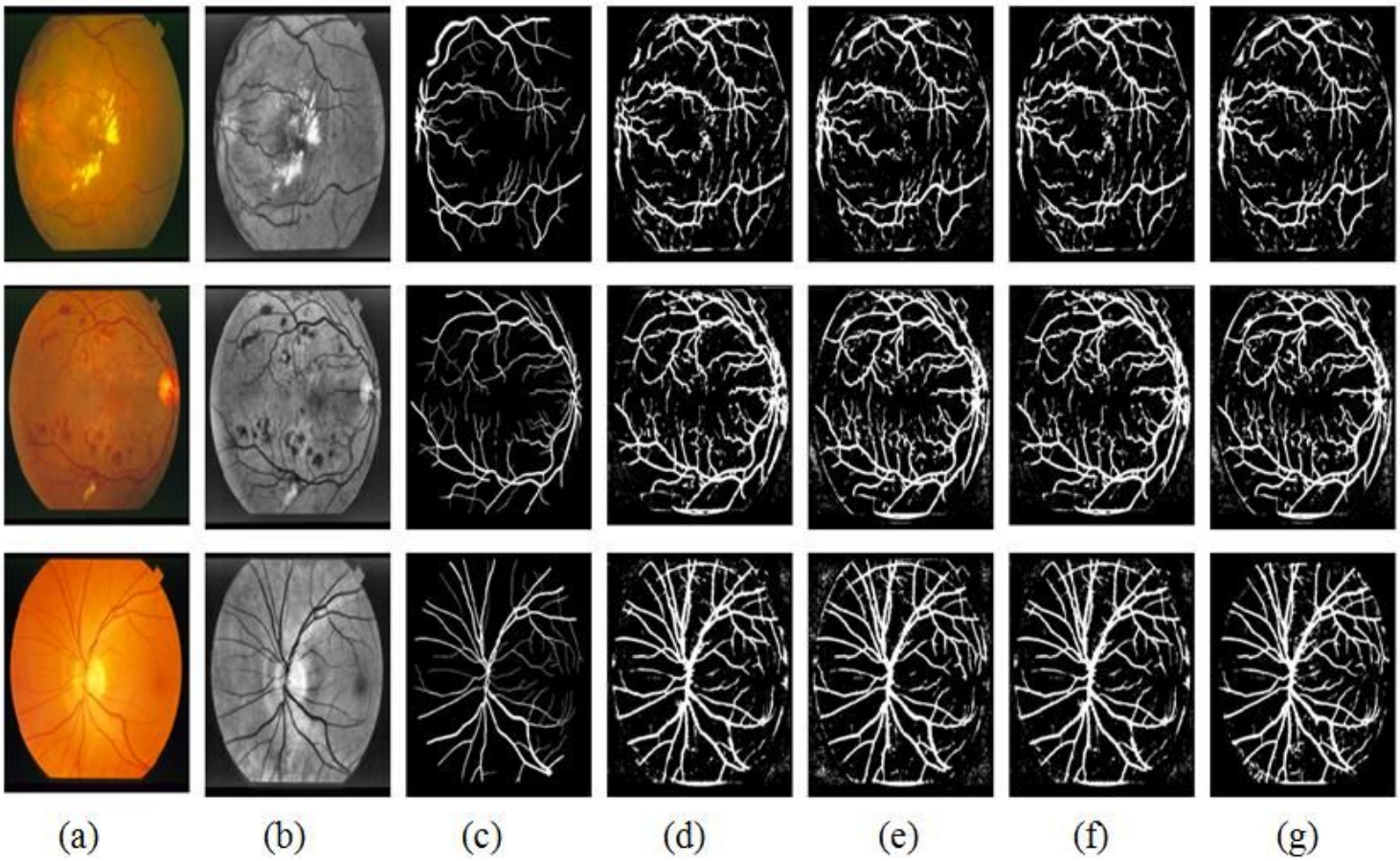

Figure 7

Segmentation result of STARE database a) Color fundus image. (b) Enhanced green channel fundus image. (c) Ground truth. (d) FCCN (e) DCNN (f) FCCN with dilation (g) DCNN dilation

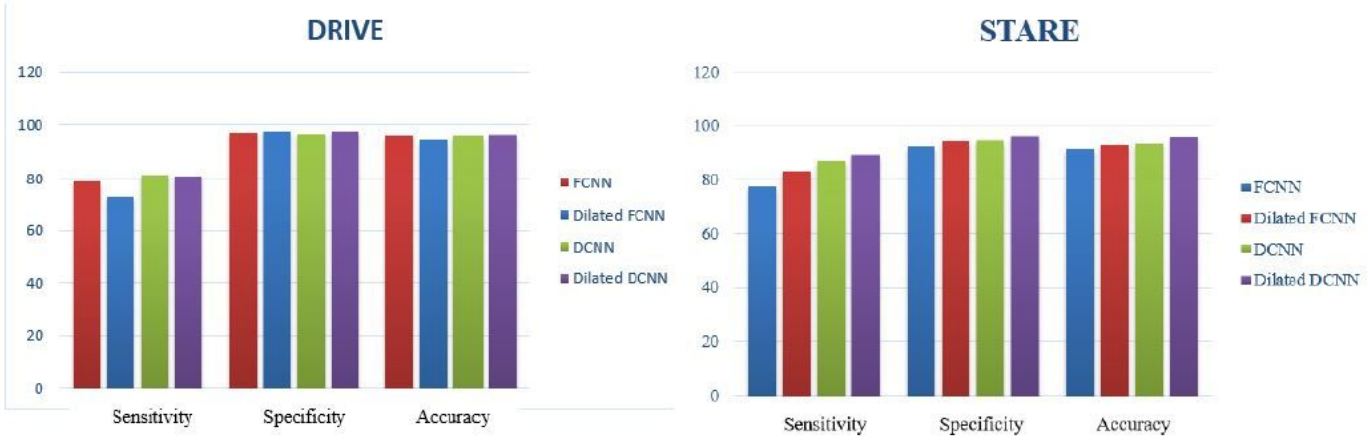

Figure 8

Bar graph comparison of evaluation metric